Ukarst : Universitas Kadiri Riset Teknik Sipil.
Volume 5 Number 1, (2021).

ISSN (*Online*) 2581-0855
ISSN (*Print*) 2579-4620

Available online at
http://ojs.unik-kediri.ac.id/index.php/ukarst/index

U KaRsT

http://dx.doi.org/10.30737/ukarst.v5i1

Accuracy of DSM By Using Unmanned Aerial Vehicles on the Downstream of Welang Riverbank, District of Pasuruan, Jawa Timur

D. W. Khaulan [1*], E. Hidayah [2], G. Halik [3].

[1 *,2,3] *Master Program in Civil Engineering, Departemen of Civil Engineering, Faculty of Engineering, University of Jember*

Email : [1*] *dean.uptti@unej.ac.id*

A R T I C L E I N F O

Article History :
Article entry : 15-10-2020
Article revised : 20-10-2020
Article received : 05-11-2020

Keywords :
Accuracy, DSM, GCP, UAV.

IEEE Style in citing this article :
[1] *S. Saksena and V. Merwade, 'Incorporating the effect of DEM resolution and accuracy for improved flood inundation mapping', J. Hydrol., vol. 530, pp. 180–194, 2015, doi: 10.1016/j.jhydrol.2015.09.069.*

A B S T R A C T

The Digital Surface Model (DSM) is commonly used in studies on flood map modeling. The lack of accurate, high-resolution topography data has hindered flood modeling. The use of the Unmanned Aerial Vehicle (UAV) can help data acquisition with sufficient accuracy. This research aims to provide high-resolution DSM-generated maps by Ground Control Points (GCPs) settings. Improvement of the model's accuracy was pursued by distributing 20 GCPs along the edges of the study area. Agrisoft software was used to generate the DSM. The generated DSM can be used for various planning purposes. The model's accuracy is measured in Root Mean Square Error (RMSE) based on the generated DSM. The RMSE values are 0.488 m for x-coordinates and y-coordinates (horizontal direction) and 0.161 m for z-coordinates (vertical direction).

1. Introduction

To model a river flood, topography data with sufficiently high resolution are necessary to represent the geometric features of the river channels and floodplains [1], [2]. However, most areas vulnerable to floods are relatively flat. A DSM generates maps containing information on elevations of all features on the Earth's surface [3], [4]. The information can then be used in flood modeling [5]. An alternative way to improve the resolution of the DSM is by generating the DSM from UAV imagery [6]. The approach of DSM generation from the UAV imagery emphasizes measurement effectiveness and accuracy [7]. It is capable of generating detailed spatial data [8], needs low cost and produces better results than DEM 30m SRTM does [9].

Ukarst : Universitas Kadiri Riset Teknik Sipil. ISSN (*Online*) 2581-0855
Volume 5 Number 1, (2021). ISSN (*Print*) 2579-4620

A number of studies has proposed ways to improve the accuracy of high-resolution DEM by using UAV imagery. The accuracy of the model can be improved by setting various variables, including the UAV flight design and the quality of the camera [10], [11], and the position of Ground Control Points [9], [12]. A previous study pursued accuracy improvement by setting the positions of Ground Control Points (GCPs) and increasing their numbers to result in low RMSE value, namely 6 cm [9]. Configuring the GCP distributions in the edges of the study area and applying stratified distribution also significantly improved the accuracy [12], [13]. The use of GCPs is important in output verification so that photogrammetry with centimeter-level accuracy can be obtained [14].

To further improve the accuracy, many authors make the use of Agrisoft software. Jebur, Abed, and Mohammed [15] used Agrisoft, and to validate the model, geometrical measurement of the shapes in the field was carried out by accurate object selection. Grisoft shows good reliability and validation in the triangulation process and in 3D modeling applications. In addition, Agrisoft Photoscan software is easier to use than LPS software because Agrisoft does not need to estimate values for unknown parameters, including exterior orientation parameters and control points [15].

This study aims to provide high-resolution Digital Surface Model (DSM) data for flood hazard mapping in flat areas. To obtain good accuracy, the DSM's construction uses UAV imagery by setting the positions of GCP to be well distributed over the study area and to be densely located on the edges of the area. The accuracy of the resulted map is quantitatively computed in Root Mean Square Error (RMSE). The mapping was conducted on seven villages in the lower course of Welding River. These villages are located close to the beach.

2. Area of Study and Method

2.1. Area of Study

The study was conducted in the lower course of Welang River, District of Pasuruan, Province of East Java as seen in figure 1. The lower course of this river has relatively flat topography, making it vulnerable to floods. A previous flood at Welang River inundated thousands of houses [16]. The total area under study is 3.31 km^2 with land covers of housings, paddy fields, and plantation field. The elevation in this area varies from 0 m to 10 m above sea level.

http://dx.doi.org/10.30737/ukarst.v3i2

ISSN (*Online*) 2581-0855
ISSN (*Print*) 2579-4620

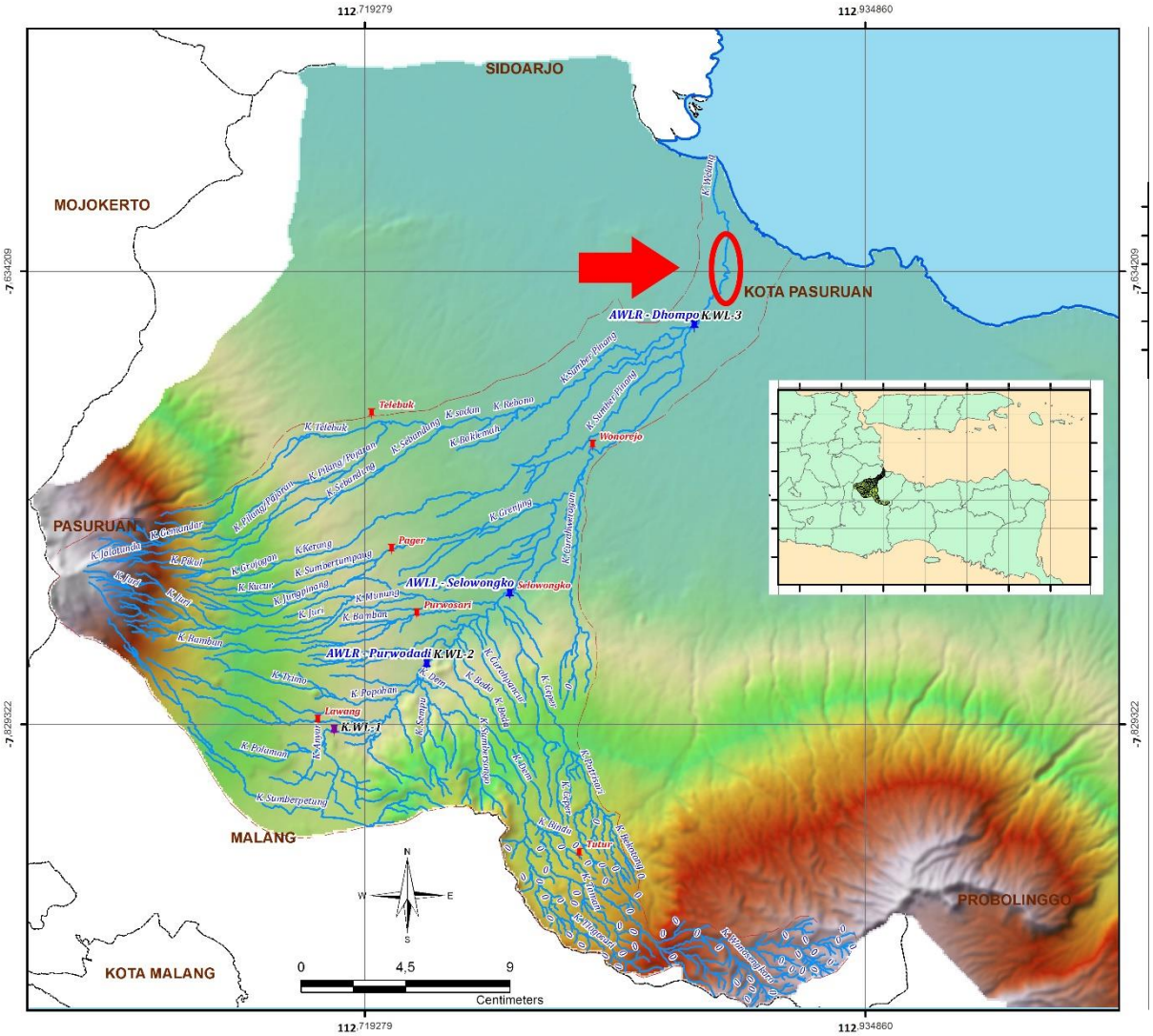

Source: UPT-PSDA Pasuruan (AutoCAD, 2020)

Figure 1. Map of the Area of Study

2.2. UAV Photogrammetry

A multi-rotor type (quadcopter) UAV, as seen in Figure 2, was used in this research. This kind of drone is commonly used in Indonesia for commercial, academic, and hobby purposes due to its relatively low cost. The UAV used in this study is a fourth-generation one, which has more sophisticated specifications than earlier generations do. Table 1 presents some of the specifications of the UAV. One of the installed features of the UAV is a forward sensor, which identifies obstacles in a forward direction so that the UAV can avoid collision during forwarding movement.

http://dx.doi.org/10.30737/ukarst.v3i2

Ukarst : Universitas Kadiri Riset Teknik Sipil. ISSN (*Online*) 2581-0855
Volume 5 Number 1, (2021). ISSN (*Print*) 2579-4620

Source: research document (Samsung note 4, 2020)

Figure 2. Quadcopter UAV technology

Table 1. Specifications of the UAV and the camera used in the research

UAV Specification		Camera Specification	
Type	Quadcopter	Sensor	CMOS 1/2,3”
Weight	1380 gram (including propellers and batteries)	Lense	FOV 94^{o} 20mm
Speed	20 m/s	Camera resolution	12.4 MP
Flight duration	28 minutes with Intelligent Flight battery of 81.3 Wh/15.2 V	Photo resolution	4000x3000 pixel
Remote control transmission distance	3.5 km	Photo format	JPEG, DNG (RAW)

Source : http://www.dji.com/phantom-4/info#specs

2.3. Settings of GCPs

The GCPs have been used to improve the accuracy of the DSM. The GCPs were distributed over the study area [11], densely located in the edges of the area to minimize the total error [12]. In this study, twenty GCPs had been located in the area prior to the UAV flight, as shown in Figure 3. The data collected by using an L1-static GPS on the land surface. The selected locations of the GCPs were permanent landmarks such as a road-corner building,

http://dx.doi.org/10.30737/ukarst.v3i2

68 - 78
ISSN (*Online*) 2581-0855
ISSN (*Print*) 2579-4620

a bridge corner, or other buildings in the area. The marks for the GCPs were painted with bright and very reflective colors, and they were well distributed in the study area. This approach was chosen to get coordinate points that can be used to assess the data's accuracy. Leica GPS used in this research has a nominal accuracy of 1 m at each of x -coordinates and y-coordinates and 2 m at z-coordinates.

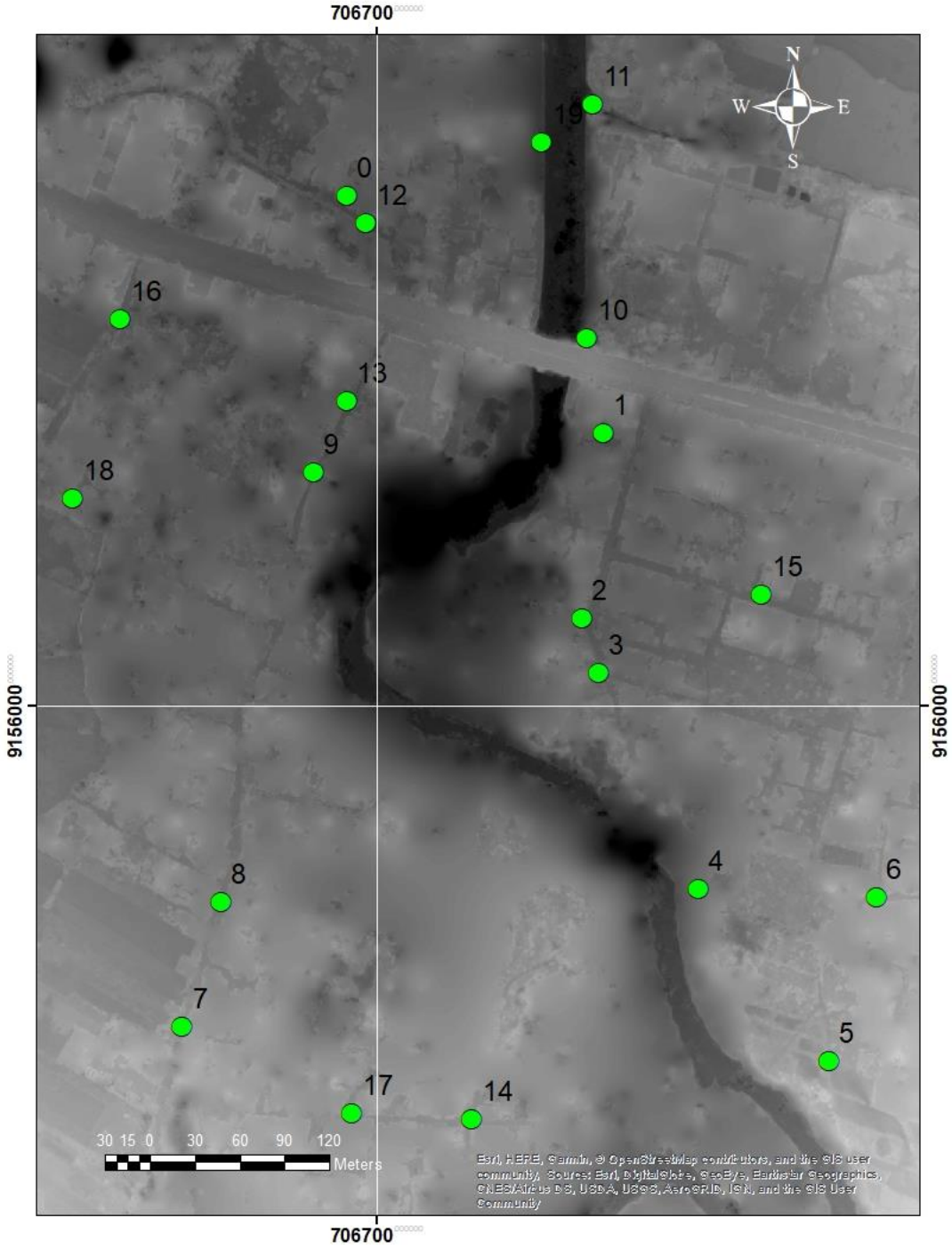

Source: Research document (Arc- GIS, 2020)

Figure 3. Positions of Ground Control Points

http://dx.doi.org/10.30737/ukarst.v3i2

Ukarst : Universitas Kadiri Riset Teknik Sipil. ISSN (*Online*) 2581-0855
Volume 5 Number 1, (2021). ISSN (*Print*) 2579-4620

2.4. DSM Map Construction

Construction of the DSM map is conducted in Agrisoft Photoscan Professional software package version 1.2.5. Agrisoft uses algorithms that have achieved significant accuracy in DSM [15]. The framework of the map construction consists of three steps. The first step was photo alignment based on feature identification and feature matching. The software estimated the orientation of the camera's external and internal parameters in the photo-alignment step, including nonlinear radial distortion. The software also estimated the required focal length, which was then extracted from the metadata. This step's results were photo positions aligned for each image, internal calibration parameters, and coordinate points. In the second step, the coordinate system in the sparse point cloud's reference settings was set to the local coordinate system (WGS84 UTM with 49S zone), and the surface type parameter of dense point cloud was set to *height field*, in accordance to the GCPs. The third step was to get the mesh exported to the DSM grid. The DSM was then used as the basis for orthorectification to produce an orthomosaic.

2.5. Accuracy Assessment

The quality of a DSM is assessed based on each pixel's accuracy, referred to as the absolute accuracy, and the accuracy of displayed morphology referred to as the relative accuracy, which is expressed in RMSE values [9], [17]. The RMSE values are computed based on the discrepancy between the observed coordinate values and the reference coordinate values. The horizontal accuracy is measured from x-coordinates and y-coordinates, and the vertical accuracy is measured from z-coordinates. Equations (1)-(3) are RMSE formulas that indicate horizontal accuracy, and equations (4)-(5) are RMSE formulas that indicate vertical accuracy.

$$\text{RMSEx} = \sqrt{\frac{\sum_{i=1}^{n}(x_{oi}-x_{ri})^2}{n}} \quad (1)$$

$$\text{RMSEy} = \sqrt{\frac{\sum_{i=1}^{n}(y_{oi}-y_{ri})^2}{n}} \quad (2)$$

$$\text{RMSExy} = \sqrt{\frac{\sum_{i=1}^{n}[(x_{oi}-x_{ri})^2+(y_{oi}-y_{ri})^2]}{n}} \quad (3)$$

$$\text{RMSEz} = \sqrt{\frac{\sum_{i=1}^{n}(z_{oi}-z_{ri})^2}{n}} \quad (4)$$

$$\text{RMSEt} = \sqrt{\text{RMSE}_{\text{xy}}{}^2 + (\text{RMSE}_{\text{z}})^2} \quad (5)$$

http://dx.doi.org/10.30737/ukarst.v3i2

70 - 78
ISSN (*Online*) 2581-0855
ISSN (*Print*) 2579-4620

With n is the number of points; x_{oi} and y_{oi} are x-coordinate and y-coordinate, respectively, that represent i-th observation (i.e. orthophoto) of the CP; x_{ri} and y_{ri} are x-coordinate and y-coordinate, respectively, that represent i-th reference (i.e. L1-static GPS measurement) of the CP. For the vertical direction, z_{oi} is the z elevation coordinate that represents i-th DSM of the CP, and z_{ri} is the z elevation coordinate that represents i-th reference (i.e. L1-static GPS measurement) of the CP.

The accuracy level of the resulted map is aimed at confirming the DSM standard accuracy that has been issued by the Indonesian Geospatial Information Agency (Badan Informasi Geospatial, BIG) [18]. According to the standard, the accuracy of x-coordinate positions and y-coordinate positions should be measured based on CE90 values, and the resolution of z-coordinate positions should be measured based on LE90. The CE90 values, associated with horizontal positions, are computed as 1.5175 times the RMSE of horizontal positions. The LE90, associated with vertical positions, are computed as 1.6499 times the RMSE of vertical positions.

3. Results and Discussion

3.1. Resulted from DSM Map

Based on IDW interpolation in Agisoft Photoscan software, 738 aligned images of the UAV (as shown in Figure 4) were exported to generate a DSM map of the study area.

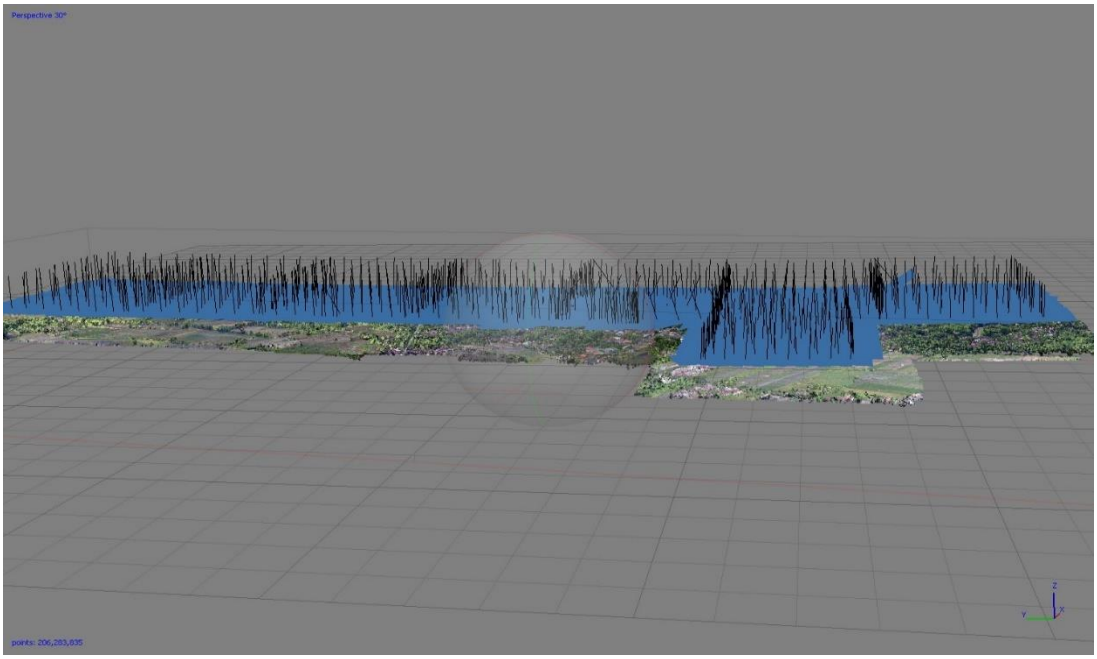

Source: Research document (Photoscan software, 2020)

Figure 4. 738 Aligned Images from the UAV Imagery

http://dx.doi.org/10.30737/ukarst.v3i2

Ukarst : Universitas Kadiri Riset Teknik Sipil. ISSN (*Online*) 2581-0855
Volume 5 Number 1, (2021). ISSN (*Print*) 2579-4620

The resulted DSM map is shown in Figure 5. The results of the DSM map, which are compared qualitatively with satellite imagery maps, show that in the red circle there is an alignment and continuity between the road lines in the province, village roads, and railways in the red circle. This shows that there is qualitative accuracy.

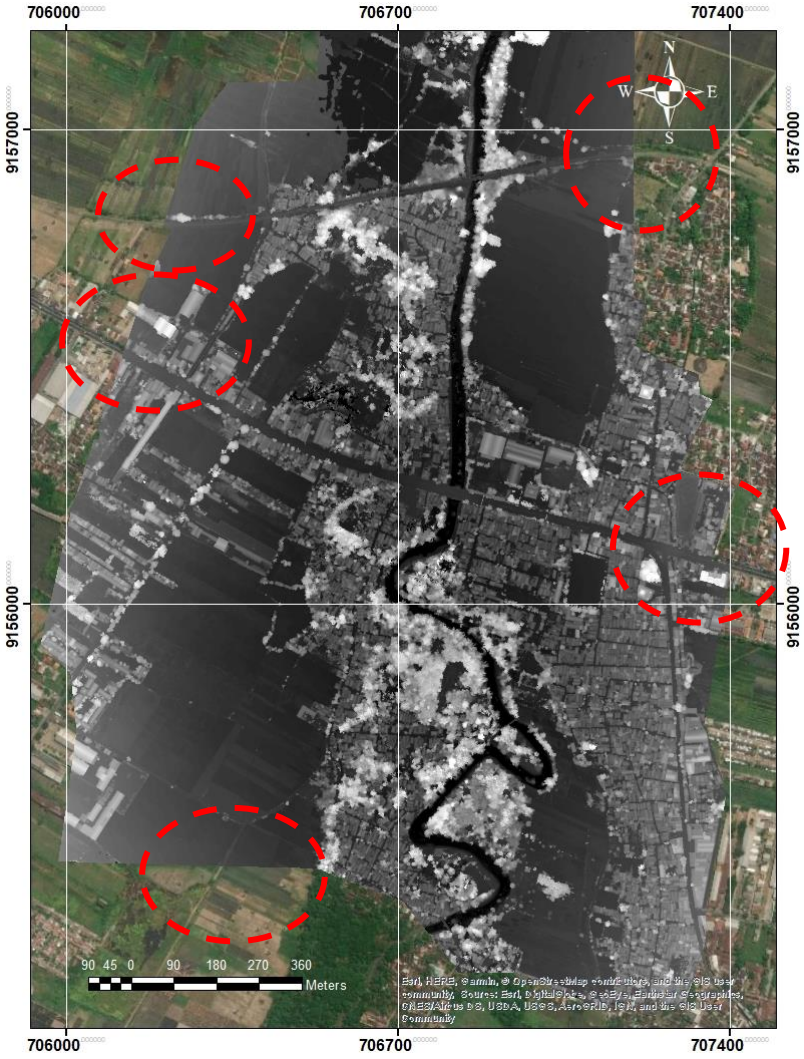

Source: Research document (Arch Gis, 2020)

Figure 5. DSM of the Area of Study

3.2. Accuracy of the DSM

Table 1 shows the values for the horizontal and vertical. The computed values of RMSE determine the quantitative accuracy of the generated DSM. RMSE values are computed from the square difference between observed coordinate values and reference coordinate values at each of 20 GCPs positions. The resulted RMSEy, computed from the sum of the square difference between the GCPs with North coordinates of observations (i.e. orthophotos) and North coordinates of the references (i.e. L1-static GPS measurement), is 0.455 m. The resulted

http://dx.doi.org/10.30737/ukarst.v3i2

72 - 78
ISSN (*Online*) 2581-0855
ISSN (*Print*) 2579-4620

RMSEx, computed from the sum of the square difference between the GCPs with East coordinates of observations (i.e. orthophotos) and East coordinates of the references (i.e. L1-static GPS measurement), is 0.488 m. The resulted RMSExy, computed by using equation (3), is 0.667 m. The resulted RMSEz is 0.161 m. It is computed from the sum of the square difference between of GCPs coordinates with observed elevations (i.e. orthophotos) and coordinates of the references (i.e. L1-static GPS measurement). The resulted $RMSE_T$ is 0.686 m. It is computed from RMSExy and RMSEz as in Equation (5). The observed coordinate points and the coordinate reference points are presented in Table 2. The resulted RMSEs are presented in Table 3.

Table 2. Horizontal and Vertical Coordinate Points

QC POIN	Reference Coordinate Points, i.e. L1-Static Measurement (m)			Observed Coordinate Points, i.e. Orthopotos (m)		
	X	Y	Z	X	Y	Z
1	706976.70	9155705	12.04	706976.20	9155704	12.14
2	706980.12	9155708	10.08	706980.97	9155708	10.21
3	706984.90	9155712	7.68	706984.86	9155713	7.73
4	706988.92	9155717	8.98	706988.08	9155716	8.64
5	706994.07	9155720	12.71	706994.58	9155720	12.89
6	706989.43	9156395	16.46	706989.05	9156396	16.63
7	706983.64	9156395	12.55	706983.10	9156396	12.49
8	706988.83	9156395	12.40	706988.10	9156394	12.51
9	706987.52	9156395	12.06	706987.16	9156395	12.53
10	706987.00	9156395	12.90	706987.20	9156395	12.87
11	706384.44	9155545	11.39	706384.92	9155546	11.39
12	706947.55	9155755	10.83	706947.95	9155754	10.87
13	706914.57	9155877	6.13	706914.61	9155878	6.14
14	706472.23	9155943	10.35	706472.23	9155942	10.46
15	706847.46	9156022	6.76	706847.94	9156023	6.68
16	706837.91	9156059	6.83	706837.35	9156059	6.71
17	706423.26	9156156	8.12	706423.54	9156156	8.28
18	706852.78	9156183	7.28	706852.17	9156184	7.28
19	706679.68	9156338	7.99	706679.26	9156339	7.87
20	706855.57	9157148	11.46	706855.21	9157147	11.44

Source: Jember University of Hydro-Technik Laboratory of (2020)

http://dx.doi.org/10.30737/ukarst.v3i2

Ukarst : Universitas Kadiri Riset Teknik Sipil. ISSN (*Online*) 2581-0855
Volume 5 Number 1, (2021). ISSN (*Print*) 2579-4620

Table 3. RMSE Values of Horizontal and Vertical Coordinate Points

Root Mean Square Error (RMSE) Validation Points
$RMSE_x$ = 0.488 m
$RMSE_y$ = 0.455 m
$RMSE_{xy}$ = 0.667 m
$RMSE_z$ = 0.161 m
$RMSE_T$ = 0.686 m

Source: Jember University of Hydro-Technik Laboratory of (2020)

The computed RMSE for z (i.e. vertical direction) is 0.161 m. By using UAVs with the same specification as the one used in this study, Akturk [9] studied 0.55 km^2 area by using 14 GCPs, and the resulted $RMSE_z$ was 0.51 m; Nagendran [14] studied 2.43 km^2 area by using 16 GCPs, and the resulted $RMSE_z$ was 0.31 m; the study of Azmi [17] resulted in $RMSE_x$ value of 0.263 m, $RMSE_y$ value of 0.412 m, and $RMSE_z$ value of 0.704 m. Compared to the previous studies that used the DJI UAVs Phanthom 3-4 series [9], [14], [17], the horizontal accuracy of this study is low, whereas the vertical accuracy of this study is high, even though the size of the mapped area in this study is bigger than those of the previous studies. The significant vertical accuracy in this study is likely a result of the GCP positioning in which the GCPs were well distributed on the study area, particularly in the edges of the area. On the other hand, the horizontal direction errors in this study are probably because the GPS used in this study was not a geodetic one. In addition, the ratio between the number of GCPs and the total measured area in this study is smaller than the ratios in the previous studies [9], [14], [17]. In principle, inaccuracies in UAVs' use depend on multifactor, such as the types of aircraft, sensors [10], operating systems, and processing software [19].

Following the computation method of the Indonesian Geospatial Information Agency's standard accuracy, it is found that on 90% confidence level, the resulting CE90 and LE90 values are 1.474 m and 0.265 m, as presented in Table 4. Therefore, based on the standard horizontal accuracy of the BIG for a base map, the class of the horizontal of the resulted map are Class 1 in 1:5000 scale, whereas the class of the vertical accuracy of the resulted map is Class 1 in 1:2500 scale. These results show that the resulting data in this study are suitable for flood hazard planning. Flood hazard mapping for the areas in the lower course of a river is an example of the DSM implementation [5], [20], [21]. Flood inundation areas are characterized by damaged topography, relatively plain, and rich of trees, so UAV imagery is extremely helpful to generate DSM for the areas.

http://dx.doi.org/10.30737/ukarst.v3i2

74 - 78
ISSN (*Online*) 2581-0855
ISSN (*Print*) 2579-4620

Table 4. DSM Accuracy and BIG Standard Accuracy

Accuracy	Test Result (m)	BIG Standard Accuracy at Scale of 1:5000		
		Class 1 (m)	Class 2 (m)	Class 3 (m)
Horizontal (CE90)	1.474	1.5	3	4.5
		BIG Standard Accuracy at Scale of 1:2500		
		Class 1 (m)	Class 2 (m)	Class 3 (m)
Vertical (LE90)	0.265	0.5	0.75	1.0

Source: Jember University of Hydro-Technik Laboratory of (2020)

http://dx.doi.org/10.30737/ukarst.v3i2

Ukarst : Universitas Kadiri Riset Teknik Sipil. ISSN (*Online*) 2581-0855
Volume 5 Number 1, (2021). ISSN (*Print*) 2579-4620

4. Conclusion and Suggestion

4.1. Conclusion

The DJI Phantom UAV DJI is good to be used for small-scale mapping. The resulting DSM map has qualitative accuracy, which indicates continuity and parallels to the satellite image map of road and railroad indicators. Geometric accuracy from this study found that the computed RMSE at x and y (i.e. horizontal direction) is 0.488 m and 0.455 m, respectively. Based on the BIG standard, the horizontal geometric accuracy is 1,474 m which is suitable for 1: 5000 scale mapping of orthophoto mosaic data. The vertical accuracy is 0.264 m which is included on the 1: 2,500 scale maps of the DSM data. This map can be used to recognize special features and details. Qualitative and quantitative (geometric) accuracy is quite detailed when used as input for modeling and mapping of coastal flood disasters

4.2. Suggestion

It is advised for future studies to achieve better accuracy, use a more advanced UAV system, improve consideration on GCP positioning, and use GPS that is both geodetic and real-time kinematic.

5. Acknowledgments

The authors are grateful to the Indonesian Ministry of Research, Technology, and Higher Education, who financially supported this research through the Postgraduate Grant program. We also thank the civil servants of the villages in the study area who granted us permission to conduct aerial photography surveys.

http://dx.doi.org/10.30737/ukarst.v3i2

76 - 78
ISSN (*Online*) 2581-0855
ISSN (*Print*) 2579-4620

References

[1] S. Saksena and V. Merwade, 'Incorporating the effect of DEM resolution and accuracy for improved flood inundation mapping', *J. Hydrol.*, vol. 530, pp. 180–194, 2015, doi: 10.1016/j.jhydrol.2015.09.069.

[2] J. Vesakoski, P. Alho, J. Hyyppä, M. Holopainen, C. Flener, and H. Hyyppä, 'Nationwide Digital Terrain Models for Topographic Depression Modelling in Detection of Flood Detention Areas', pp. 271–300, 2014, doi: 10.3390/w6020271.

[3] I. Indarto and D. Prasetyo, 'Pembuatan Digital Elevation Model Resolusi 10m dari Peta RBI dan Survei GPS dengan Algoritma ANUDEM', *J. Keteknikan Pertan.*, vol. 2, no. 1, p. 21955, 2014.

[4] A. N. Safi'i and P. Hartanto, 'Pembuatan Digital Terrain Model (DTM) dari Light Detection and Ranging (LiDAR) menggunakan Metode Morfologi Sederhana', *Teknik*, vol. 40, no. 1, p. 40, 2019, doi: 10.14710/teknik.v40i1.23004.

[5] S. Mourato, P. Fernandez, L. Pereira, and M. Moreira, 'Improving a DSM Obtained by Unmanned Aerial Vehicles for Flood Modelling', *IOP Conf. Ser. Earth Environ. Sci.*, vol. 95, no. 2, 2017, doi: 10.1088/1755-1315/95/2/022014.

[6] A. Jebur, F. M. Abed, and M. U. Mohammed, '3D City Modelling by Photogrammetric Techniques', no. July 2019, 2017, doi: 10.13140/RG.2.2.11494.06722.

[7] N. Arsyad, 'Akurasi Citra data Foto Udara Persimpangan Lalu Lintas Kota Kendari', *Rekayasa Sipil*, vol. 14, no. 1, pp. 51–59, 2020.

[8] R. Meiarti, T. Seto, and J. Sartohadi, 'Uji Akurasi Hasil Teknologi Pesawat Udara Tanpa Awak (Unmanned Aerial Vehicle) Dalam Aplikasi Pemetaan Kebencanaan Kepesisiran', *J. Geogr. Edukasi dan Lingkung.*, vol. 3, no. 1, p. 1, 2019, doi: 10.29405/jgel.v3i1.2987.

[9] E. Akturk and A. O. Altunel, 'Accuracy assesment of a low-cost UAV derived digital elevation model (DEM) in a highly broken and vegetated terrain', *Meas. J. Int. Meas. Confed.*, vol. 136, no. February 2019, pp. 382–386, 2019, doi: 10.1016/j.measurement.2018.12.101.

ISSN (*Online*) 2581-0855
ISSN (*Print*) 2579-4620

[10] A. R. Yusoff, M. F. Mohd Ariff, K. M. Idris, Z. Majid, and A. K. Chong, 'Camera calibration accuracy at different UAV flying heights', *Int. Arch. Photogramm. Remote Sens. Spat. Inf. Sci. - ISPRS Arch.*, vol. 42, no. 2W3, pp. 595–600, 2017, doi: 10.5194/isprs-archives-XLII-2-W3-595-2017.

[11] E. Sanz-Ablanedo, J. H. Chandler, J. R. Rodríguez-Pérez, and C. Ordóñez, 'Accuracy of Unmanned Aerial Vehicle (UAV) and SfM photogrammetry survey as a function of the number and location of ground control points used', *Remote Sens.*, vol. 10, no. 10, 2018, doi: 10.3390/rs10101606.

[12] P. Martínez-Carricondo, F. Agüera-Vega, F. Carvajal-Ramírez, F. J. Mesas-Carrascosa, A. García-Ferrer, and F. J. Pérez-Porras, 'Assessment of UAV-photogrammetric mapping accuracy based on variation of ground control points', *Int. J. Appl. Earth Obs. Geoinf.*, vol. 72, no. May, pp. 1–10, 2018, doi: 10.1016/j.jag.2018.05.015.

[13] V. Casella, F. Chiabrando, M. Franzini, and A. M. Manzino, 'Accuracy assessment of a UAV block by different software packages, processing schemes and validation strategies', *ISPRS Int. J. Geo-Information*, vol. 9, no. 3, 2020, doi: 10.3390/ijgi9030164.

[14] S. K. Nagendran, W. Y. Tung, and M. A. Mohamad Ismail, 'Accuracy assessment on low altitude UAV-borne photogrammetry outputs influenced by ground control point at different altitude', *IOP Conf. Ser. Earth Environ. Sci.*, vol. 169, no. 1, 2018, doi: 10.1088/1755-1315/169/1/012031.

[15] A. Jebur, F. Abed, and M. Mohammed, 'Assessing the performance of commercial Agisoft PhotoScan software to deliver reliable data for accurate3D modelling', *MATEC Web Conf.*, vol. 162, 2018, doi: 10.1051/matecconf/201816203022.

[16] M. A.- DetikNews, '8.740 Rumah di 9 Desa/Kelurahan di Pasuruan Terendam Banjir', [Online]. Available: https://news.detik.com/berita-jawa-timur/d-3880153/8740-rumah-di-9-desakelurahan-di-pasuruan-terendam-banjir.

[17] S. M. Azmi, B. Ahmad, and A. Ahmad, 'Accuracy assessment of topographic mapping using UAV image integrated with satellite images', *IOP Conf. Ser. Earth Environ. Sci.*, vol. 18, no. 1, 2014, doi: 10.1088/1755-1315/18/1/012015.

[18] Badan Informasi Geospasial, *PERATURAN BADAN INFORMASI GEOSPASIAL NOMOR 6 TAHUN 2018*. 2018.

http://dx.doi.org/10.30737/ukarst.v3i2

ISSN (*Online*) 2581-0855
ISSN (*Print*) 2579-4620

[19] G. Popescu, D. Iordan, and V. Păunescu, 'The Resultant Positional Accuracy for the Orthophotos Obtained with Unmanned Aerial Vehicles (UAVs)', *Agric. Agric. Sci. Procedia*, vol. 10, pp. 458–464, 2016, doi: 10.1016/j.aaspro.2016.09.016.

[20] E. Yalcin, 'Two-dimensional hydrodynamic modelling for urban flood risk assessment using unmanned aerial vehicle imagery: A case study of Kirsehir, Turkey', *J. Flood Risk Manag.*, vol. 12, no. S1, pp. 1–14, 2019, doi: 10.1111/jfr3.12499.

[21] C.-G. Jung and S.-J. Kim, 'Comparison of the Damaged Area Caused by an Agricultural Dam-Break Flood Wave Using HEC-RAS and UAV Surveying', *Agric. Sci.*, vol. 08, no. 10, pp. 1089–1104, 2017, doi: 10.4236/as.2017.810079.